

# TMCI with Resonator Wakes

A. Burov\* and T. Zolkin

Fermilab, PO Box 500, Batavia, IL 60510-5011

(Dated: March 21, 2022)

Transverse mode-coupling instability (TMCI) with a high-frequency resonator wake is examined by the Nested Head-Tail Vlasov solver (NHT), where a Gaussian bunch in a parabolic potential (GP model) is represented by concentric rings in the longitudinal phase space. It is shown that multiple mode couplings and decouplings make impossible an unambiguous definition of the threshold, unless Landau damping is taken into account. To address this problem, instead of a single instability threshold, an interval of thresholds is suggested, bounded by the low and high intensity ones. For the broadband impedance model, the high intensity threshold is shown to follow Zotter's scaling, but smaller by about a factor of two. The same scaling, this time smaller than Zotter's by a factor of four, is found for the ABS model (Air Bag Square well).

## I. INTRODUCTION

In principle, there are two distinct approaches to beam stability problems: the beam can be represented by a set of either macroparticles or continuous objects. The first choice leads to macroparticle tracking simulations, while the second one is applied in Vlasov solvers. Each of the methods has its advantages and drawbacks. The main advantage of the macroparticle approach lies in its potential to be closer to reality. This closeness may require, though, a lot of macroparticles, i.e. a lot of CPU time, which is a serious drawback. Vlasov solvers can be many orders of magnitude faster than typical macroparticle programs, but it remains to be unresolved how to include there, with accuracy and effectiveness, such factors as the space charge, certain kinds of Landau damping, or the electron cloud.

This paper deals with a problem where Vlasov solvers apparently demonstrate their power in full: the transverse mode coupling instability (TMCI) without space charge. This instability used to be considered as one with a sharp threshold, i.e. which growth rate rapidly increases with the bunch intensity above its certain threshold value. That sort of TMCI behavior was demonstrated for the non-resonant wake functions, like the resistive wall one, possibly accompanied by a damper, see ref. [1, 2]. If the calculated threshold is sharp, even a strong variation of the Landau damping may only slightly change the onset of the instability, thus justifying the omission of the Landau damping in the threshold computation. A question may be asked though: is the TMCI threshold always as sharp as for the resistive wall type wakes? This question is especially motivated for short or highly oscillating wakes within the bunch length, where multiple mode couplings and decouplings may be important. Being driven by these questions, we limit our consideration here by high-frequency resonator wakes, i.e. by those which wavelength is shorter than the bunch length.

Using NHT Vlasov solver [1], it is shown below that

the TMCI threshold is not actually sharp for the high-frequency wakes: as the bunch intensity begins to increase, the first couplings that appear are weak, being soon followed by the decouplings. With further increase of the intensity, mode couplings become stronger, with higher growth rates and larger coupling-decoupling intervals. As a result, the growth rate rises rather gradually with the intensity, making the very concept of the *TMCI threshold* vague unless the Landau damping is specified. Such sort of instability, with a cascade of the thresholds, was observed at the SPS, see e.g. Refs. [3, 4].

To deal with this conceptual uncertainty, the TMCI threshold can be represented by two intensities, low and high, with the former showing the first, very weak, mode coupling, and the latter pointing to a case where the growth rate increases sharply, soon after its appearance becoming comparable with the synchrotron tune. The asymptotical scaling of the high-intensity threshold is found in agreement with estimations of B. Zotter [5] and E. Metral [6], with a difference of numerical coefficients by a factor of  $\sim 2$ .

A sensitivity of the TMCI thresholds to the shape of the potential well was examined by comparison of the Gaussian bunch in the parabolic bucket with the air-bag bunch in the square well. For the latter, we used Blaskiewicz' model as implemented in Ref. [7]. Reasonable agreement of the two models is demonstrated.

## II. PARABOLIC POTENTIAL WELL

The resonator wake function can be presented as

$$W(\tau) = W_0 \sin(\hat{\omega} \tau) e^{\omega_r \tau / (2 Q_r)}; \quad W_0 = R_s \frac{\omega_r^2}{\hat{\omega} Q_r}, \quad (1)$$

where  $R_s$  is the transverse shunt impedance, frequency of oscillation

$$\hat{\omega} = \sqrt{\omega_r^2 - \alpha^2}, \quad (2)$$

and the decay rate related to the resonant frequency  $\omega_r$  by means of the  $Q$ -factor  $Q_r$ :

$$\alpha = \omega_r / (2 Q_r). \quad (3)$$

---

\* burov@fnal.gov

At zero chromaticity, assumed at this paper, the problem is expressed in terms of the following dimensionless parameters:

$$\chi = \frac{N_p r_0 R_0 W_0}{4\pi\gamma\beta^2 Q_\beta Q_s} = \frac{N_p r_0}{\gamma\beta Q_\beta \omega_s} \frac{R_s \omega_r^2}{Z_0 Q_r \hat{\omega}} \quad (4)$$

$$\psi_r = \omega_r \sigma_\tau \equiv 2\pi\nu_r; \quad \Delta_r = \alpha\sigma_\tau. \quad (5)$$

Here  $Z_0 = 4\pi/c = 377\Omega$ ,  $r_0$  is the particle classical radius,  $N_p$  is the number of particles per bunch,  $\sigma_\tau$  is the rms bunch length,  $R_0 = C_0/(2\pi)$  is the average accelerator ring radius,  $Q_\beta$  is the betatron tune,  $Q_s$  and  $\omega_s$  are the synchrotron tune and angular frequency,  $\gamma$  and  $\beta$  are the Lorentz factors.

An important motivation for this paper was understanding of the instability at CERN SPS, where the threshold was both measured and computed. Assuming the high frequency resonator wake, the latter has been done with the MOSES Vlasov solver and the HEAD-TAIL tracking [3, 8] for the old Q26 lattice, and recently repeated for the new Q20 optics in the tracking simulations [9]. A surprising result of all the computations, both old and new, was nearly complete independence of the threshold on the space charge. In order to understand that, a more detailed look at the instability without the space charge for the high frequency broadband impedance model is needed as the first step. To make it easier, we are presenting our results in terms of the threshold number of particles per bunch  $N_p$ , assuming the SPS optics Q20 with the gamma transition  $\gamma_t = 18$ , at injection energy 26GeV, the synchrotron tune  $Q_s = 0.017$  and the rms bunch length  $\sigma_s = c\sigma_\tau = 23$  cm. In terms of the dimensionless  $\chi$  parameter, Eq. (4), the relation between that and the number of particles can be presented as:

$$\chi = 10 \frac{N_p}{10^{11}} \frac{\omega_r}{2\pi \cdot 1.3\text{GHz}} \frac{R_s}{7\text{M}\Omega/\text{m}} \sqrt{\frac{3}{4Q_r^2 - 1}}. \quad (6)$$

Let's start from the SPS impedance model of the broadband resonance at  $f_r = \omega_r/(2\pi) = 1.3\text{GHz}$ ,  $Q_r = 1$  and  $R_s = 7\text{M}\Omega/\text{m}$ , with the air-bag approximation. The bunch modes for various intensities are presented in Fig. 1.

The air-bag model works with variations of the dipole moment along the synchrotron phase; it does not take into account the variations along the synchrotron action, the so called radial harmonics. In the NHT Vlasov solver, any number of the radial rings can be taken to represent the bunch phase space distribution; thus, the radial harmonics can be included.

Figures 2 and 3 show how sensitive the instability is to the radial degrees of freedom. Both plots describe the same bunch and impedance as the air-bag, Fig. 1, but with more accuracy, taking 5 and 10 radial rings respectfully, as well as double the azimuthal harmonics. Although there is some visible difference between Figs.

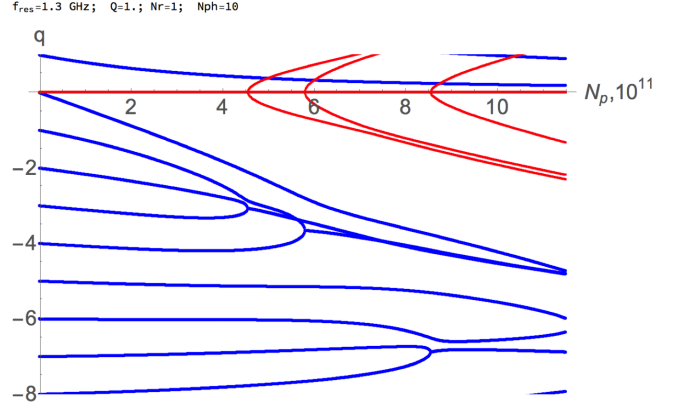


FIG. 1. Bunch modes versus the number of particles for the SPS at injection and Q20 optics. Coherent tunes  $q$  are given in units of the synchrotron tune; real and imaginary parts are blue and red respectively. The resonator impedance is taken with  $f_r = \omega_r/(2\pi) = 1.3\text{GHz}$ ,  $Q_r = 1$  and  $R_s = 7\text{M}\Omega/\text{m}$ . The bunch distribution is represented by a single ring in the longitudinal phase space, which is the air-bag model, with the radius  $\sqrt{2}\sigma_s$ . The head-tail harmonics are truncated at  $\pm 10$ . The resonant frequency, Q-factor, number of rings and head-tail truncation number are noted above the plot.

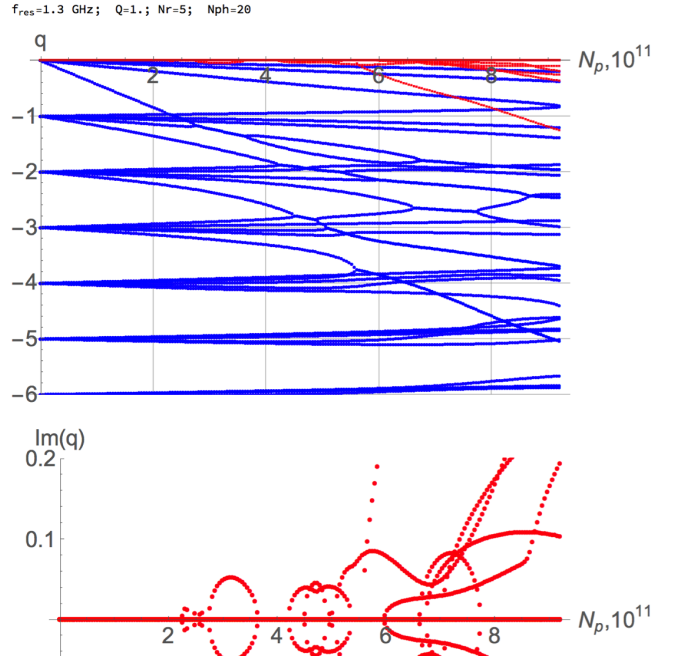


FIG. 2. Same as Fig. 1, but with 5 NHT rings and head-tail truncation at  $\pm 20$ .

2 and 3, their main features are similar, so we may reasonably consider them converged, and compare them together, as the many-ring case, the Gaussian bunch in the Parabolic bucket (GP model), with the air-bag case. Below we itemize some features of these plots.

- For many rings the mode couplings begin at about

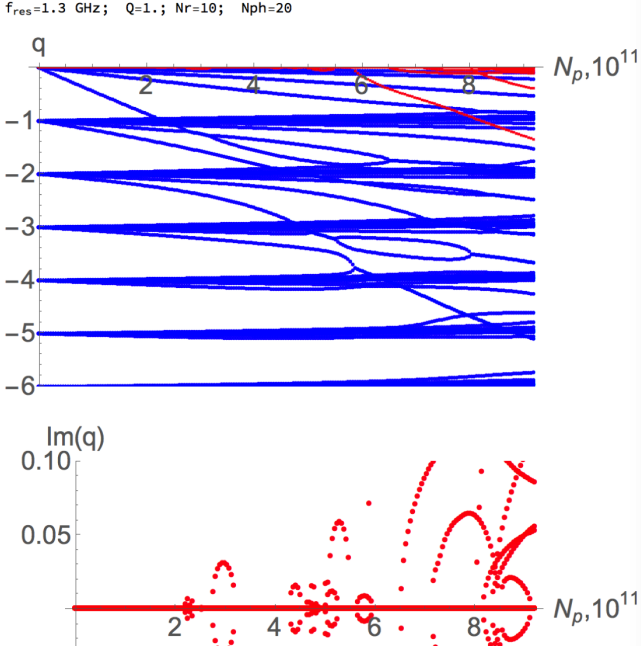


FIG. 3. Same, but with 10 NHT rings and head-tail truncation at  $\pm 20$ .

factor of 2 lower intensity than for the air-bag (ABP) model. The first couplings are weak, soon followed by the decouplings and new, stronger, couplings. In this way, the instability growth rate goes up and down, increasing on the average. Similar mode behavior was recently observed with GALACTIC Vlasov solver for the broadband impedance with  $\nu_r = 0.7$  [10].

- The intensity spread between the weak and strong couplings is about factor of 3 for these parameters. Without sufficient knowledge of the Landau damping, the real onset of the instability can be predicted only with that poor accuracy.
- Coupling of the negative 2nd and 3rd azimuthal harmonics happens at the intensity of  $N_p = 4.5 \cdot 10^{11}$ , in agreement with the pyHEADTAIL macroparticle tracking simulations [11]. Figure 3 suggests that for those simulations, the effective Landau damping rate was as small as  $\leq 0.05\omega_s$ .

How does the instability depend on the wake  $Q$ -value,  $Q_r$ ? Some information on that is suggested by Figs. 4, 5 and 6, which show the modes computed for the same shunt impedance and resonator frequency, but doubled  $Q_r$ . Comparing these plots with the previous three, we may conclude that in this case the thresholds increased twofold, as the  $Q$ -value. It is worth to note that with higher  $Q_r$ , convergence requires more rings.

Figs. 7, 8 illustrate how the instability depends on the resonator frequency  $\omega_r$ . Comparing them with the corresponding plots for half the resonator frequency, we may

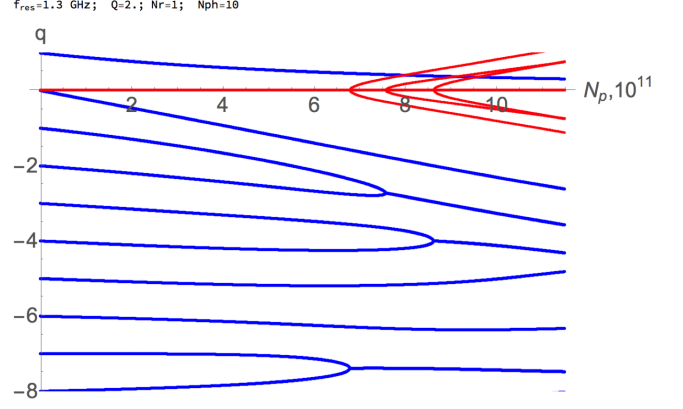


FIG. 4. Same shunt impedance and frequency, but  $Q_r = 2$ . Air-bag, head-tail truncation at  $\pm 10$ .

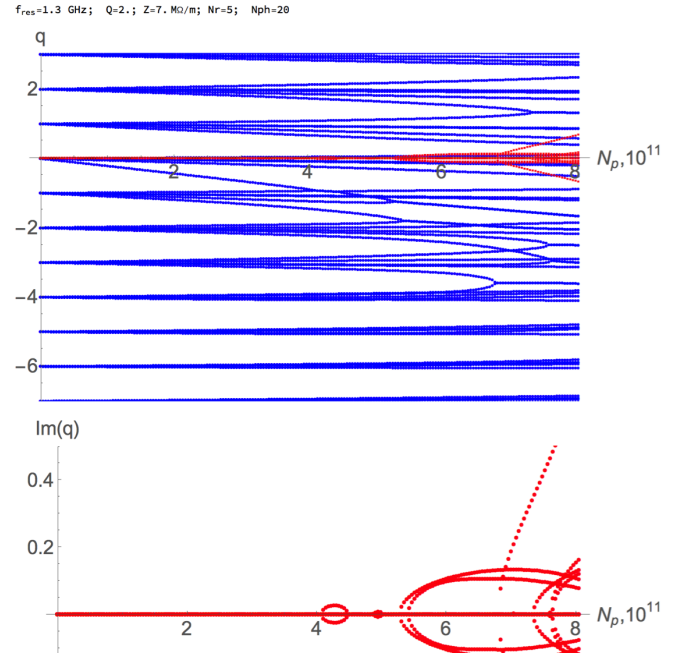


FIG. 5. Same, with 5 rings and truncation at  $\pm 20$ . Note that the positive modes may also couple, but this does not play a significant role.

conclude that while the air-bag and low-intensity thresholds are almost the same, the high-intensity threshold for the multi-ring GP model is doubled for double the frequency.

Looking at Figs. 3, 6, one may guess that the thresholds will show proportionality to the  $Q$ -value for higher resonator frequency as well. However, comparison of Fig. 9 with Fig. 8, show that it is not necessarily so: the two plots demonstrate almost the same high-intensity threshold, while their  $Q$ -values differ by the factor of two.

The presented plots convince the authors that there is no good analytical fitting for the TMCI threshold versus frequency and  $Q$ -value for high-frequency resonator

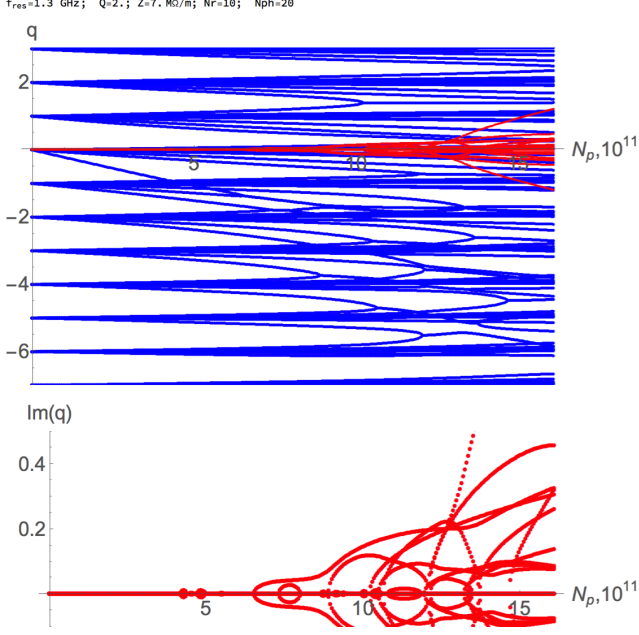
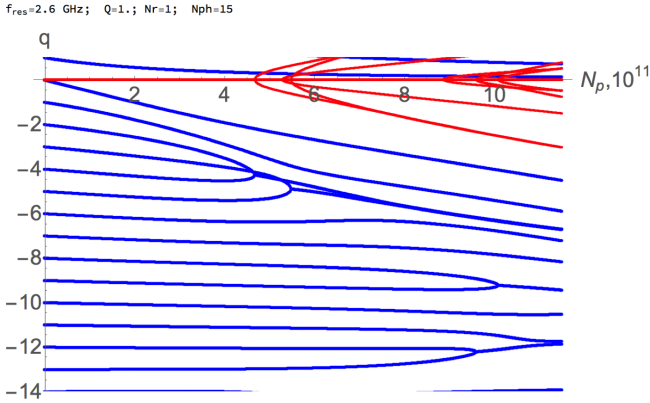


FIG. 6. Same, with 10 rings.

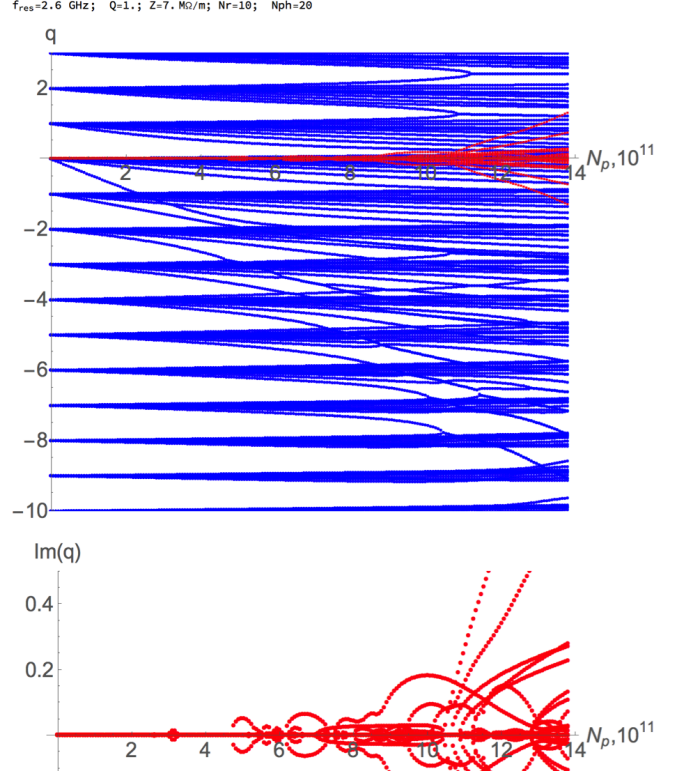
FIG. 7. The resonator frequency is doubled,  $f_r = 2.6\text{GHz}$ , the shunt impedance is the same,  $Q_r = 1$ , air-bag, head-tail truncation at  $\pm 15$ .

wake,  $\omega_r \sigma_\tau \gg 1$ , for the considered range of parameters. After all, there is no reason for that: in this sort of computation, finding the minimum of several functional branches is involved; taking the minimum is not an analytical procedure.

What about the air-bag approximation? Can it be considered a reasonable way to estimate the instability threshold? Plots of the air-bag thresholds versus the wake phase advance  $\nu_r = f_r \sigma_\tau$  for various  $Q$ -values are presented in Fig. 11. They demonstrate that for  $Q_r = 1$ , the fitting formula

$$\chi_{\text{th}}^{\text{ABP}} = 40\nu_r \quad (7)$$

works well; for all  $Q$ -values this linear dependence works better than other powers of  $\nu_r$ . In terms of the number

FIG. 8. Same as the previous Figure, but with 10 rings and the truncation at  $\pm 20$ .

of particles, it is equivalent to the threshold  $N_{\text{th}}$  being independent of the wake frequency  $f_r$  when the shunt impedance  $R_s$  is given; for  $Q_r = 1$ :

$$N_{\text{th}}^{\text{ABP}} = 6 \frac{\gamma \beta Q_\beta \omega_s \sigma_\tau}{r_0} \frac{Z_0}{R_s}. \quad (8)$$

Such dependence means that only an integral of the wake, i.e. the shunt impedance, is important for the threshold number of particles. Figure 10 demonstrates that for even an higher frequency of 10.4 GHz, the threshold is still the same, albeit the numbers of the coupling modes are larger. This leads us to the conclusion that the same threshold has to be expected for the delta-function wake,  $W(\tau) = R_s \delta(\tau)$ . On another hand, it can be proven that the delta-wake cannot lead to any instability of a thermalized bunch, independently of the potential well. Indeed, the delta-wake is equivalent to a combination of the space charge and longitudinally-dependent external transverse focusing, so the system can be described by a time-independent Hamiltonian. Such systems in thermal equilibrium must be stable: the opposite would violate the Second Law of Thermodynamics. Thus, the instability threshold of Eq. (8) may follow only from the inadequacy of the ABP model for the Gaussian bunch, where such dependence shouldn't be possible. The phase space density of the air-bag approximation is a highly non-monotonic function of the longitudinal action; moreover, at the bunch edges,  $\tau = \pm \tau_b/2 \equiv \hat{\tau}$ , the

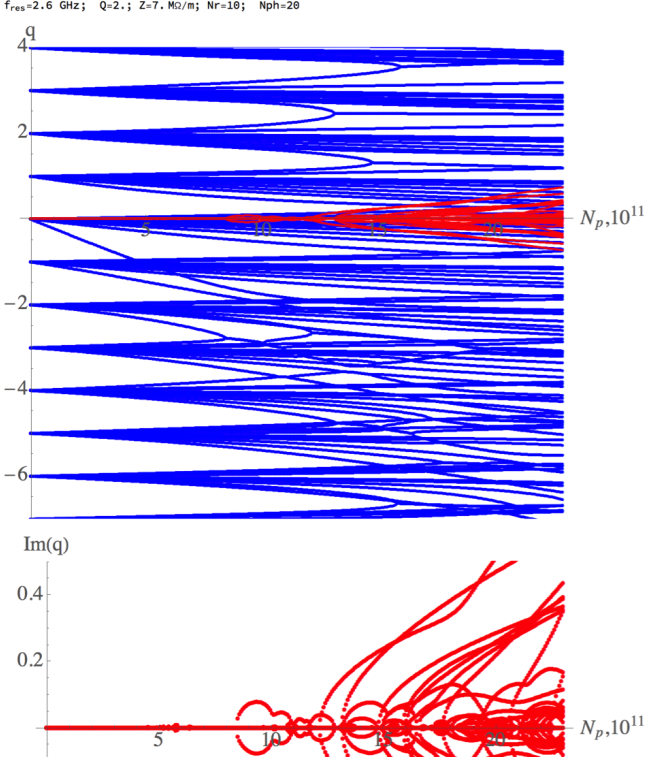


FIG. 9.  $f_r = 2.6\text{GHz}$ ,  $Q_r = 2$ .

ABP line density has singularities  $\sim 1/\sqrt{\hat{\tau}^2 - \tau^2}$ . Those unphysical properties of the ABP model may be reasonably tolerable for long-range wake functions  $\nu_r \ll 1$ , but they lead to inadequate results for the short-range ones,  $\nu_r \geq 1$ , when the role of the line density singularities is more pronounced. This conclusion is supported by comparison of Figs. 3 and 8, taken for doubled wake frequencies and computed with the sufficient number of the rings. While the air-bag model gives the same threshold number of particles for the two cases, the multi-ring GP model points to the increase of both low and high intensity thresholds. The most interesting of them, the latter, increases by about a factor of 2, proportionally to the frequency. Led by this observation, one may suggest the following high-intensity threshold for  $Q_r = 1$ :

$$\chi_h = 60\nu_r^2. \quad (9)$$

or

$$N_h = 1.5 \frac{\gamma Q \beta \omega_s \omega_r \sigma_\tau^2}{r_0} \frac{Z_0}{R_s}, \quad (10)$$

where the subscript  $h$  stands for *high*.

The frequency scaling of Eq.(10) agrees with one predicted by B. Zotter [5] and E. Metral [6], while their numerical factors are about two times larger. On another hand, as shown in the next section, the high intensity GP instability threshold (10) exceeds by factor of 2 the high-frequency asymptote of the TMCI threshold for

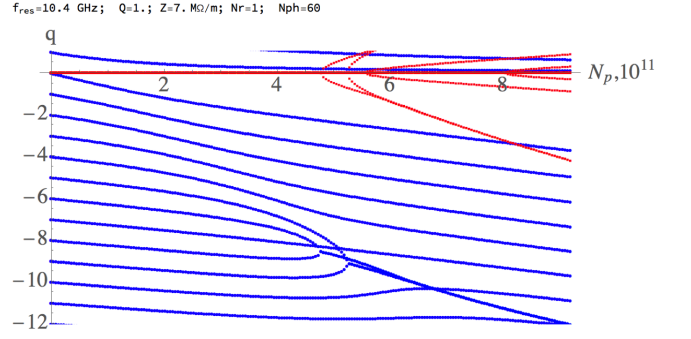


FIG. 10. Air-bag with 10.4GHz wake, same  $R_s$  and  $Q_r = 1$ . Although the threshold is same as for the lower frequency, the coupling mode numbers are higher.

the ABS model. Elias Metral drew our attention to an article of J.-L. Laclare [12], where the TMCI threshold for high-frequency broadband impedance was independently calculated. It was proposed by Metral, that there is a typo in the vertical axis label of the last Laclare's plot, Fig. (37): instead of  $\varepsilon_{th} Z_\perp p_r B_0$  there must be just  $\varepsilon_{th} Z_\perp$ . Indeed, the numbers in the textual surrounding of this plot confirm this guess very well. A possible reason for that sort of typo might be just lost round brackets, closing  $p_r B_0$  as the argument. Following this guess, one may express the linear high-frequency dependence of Laclare's Fig. (37) in terms of this paper, and obtain our Eq. (10) with just slightly higher numerical factor, 1.7, instead of our 1.5.

It's interesting that Zotter's scaling (10) is identical to one of the coasting beam, as it was noted by E. Metral; this becomes obvious after a substitution  $\omega_s \sigma_\tau^2 = |\eta| \epsilon_z / (\gamma \beta^2 m c^2)$ , where  $\eta$  is the slippage factor and  $\epsilon_z$  is the rms longitudinal emittance. If this agreement is not a coincidence, the same scaling would be valid rather independently of the  $Q$ -value. Our current data and understanding of the issue does not allow us making a definite statement on that.

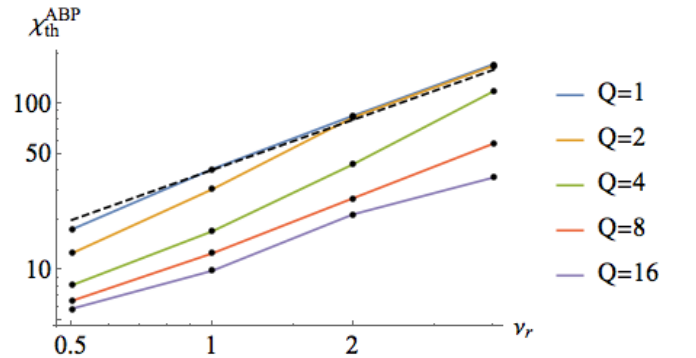


FIG. 11. Threshold  $\chi$  parameters for the ABP model versus the phase advance  $\nu_r = f_r \sigma_\tau$  at various  $Q$ -values. The dashed line is a linear fit  $\chi_{th}^{ABP} = 40\nu_r$  for  $Q_r = 1$ .



The low-intensity threshold can be fitted as

$$\chi_l = 20\nu_r; \quad N_l = 3 \frac{\gamma\beta Q_\beta \omega_s \sigma_\tau}{r_0} \frac{Z_0 Q_r}{R_s}, \quad (11)$$

with the subscript  $l$  standing for *low*. For  $Q_r = 1$ , the two thresholds merges at  $\omega_r \sigma_\tau \approx 2$ . For the SPS Q20 parameters it corresponds to  $f_r = 0.45$  GHz. According to that, the TMCI threshold must be sharp at frequency below this value. Figure 12 confirms that, showing the spectra slightly above this high-low merge, when the intensity interval between them is almost zero. Although the low-intensity threshold (11) has the same scaling as the ABP one (8), the former does not necessarily contradict to the Second Law of Thermodynamics in the sense as the latter does. Indeed, with increase of the wake frequency, the instability growth rate at the low-intensity edge may become smaller and smaller, which tendency is confirmed by the presented plots.

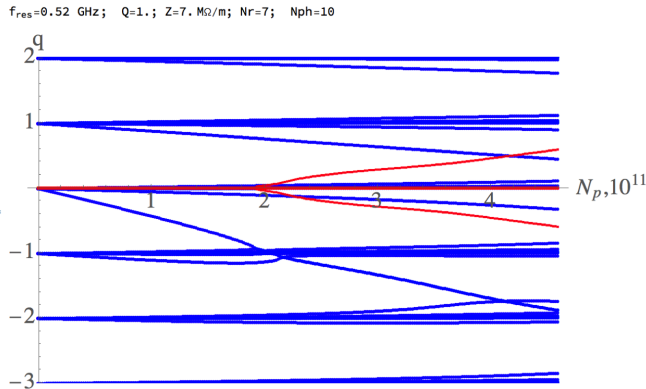


FIG. 12. The spectrum at the resonator frequency just slightly above the high-low merge,  $\nu_r = 0.4$ . Note the tiny intensity interval between a weak and a strong coupling of the mode 0 with different modes  $-1$ . Below this frequency, the TMCI threshold is sharp.

### III. SQUARE POTENTIAL WELL

How sensitive are the thresholds to the potential well shape? In order to shed light on that, we consider a bucket rather dissimilar to the parabolic one: the square well. The analysis in the previous section forced us to conclude that the air-bag model is not a good representative of a Gaussian-like bunch in the parabolic potential well. However, this conclusion is not necessarily valid for the square well, where the line density never goes to infinity. The possibility of an exact analytical solution with an arbitrary space charge and any combination of the resonator wakes, demonstrated by M. Blaskiewicz [13], suggests that the air-bag bunch in the square well may be particularly interesting. Led by this interest, we consider here the instability for the air-bag distribution in a square well, the ABS model, following the same routine as we recently have [7]. A space charge of zero is

assumed here; instead, we vary the wake frequency and  $Q$ -value and study how the instability threshold changes with that. Our main task here is to see the level of agreement between the GP and the ABS models.

For that, we take the total length of the ABS bunch,  $\tau_b$ , equal to three rms lengths of the GP case:  $\tau_b = 3\sigma_\tau$ . With this convention, the SPS wake model with  $f_r = 1.3$  GHz results in the ABS phase advance  $f_r \tau_b = 3\nu_r = 3$ . Figure 13 shows the coherent spectra for this and doubled resonator frequencies. Their comparison demonstrates that the numbers of the coupled modes grow linearly with the wake frequency, as  $2f_r \tau_b$ . This is different from the GP case, where, as it was shown above, a series of couplings and decouplings were observed, where the instability rate increased on average with the bunch intensity.

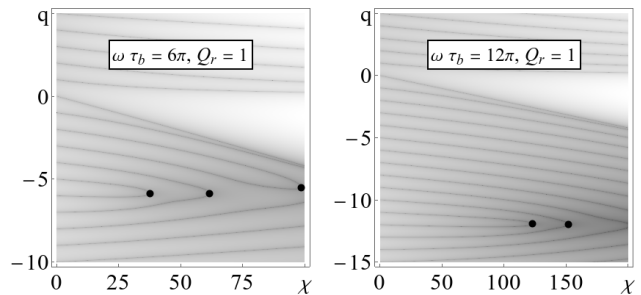


FIG. 13. Collective spectra for the ABS model. Only real tunes are shown; the mode couplings are marked by dots. Comparison of the left and right plots show that when the wake frequency doubles, numbers of the coupling modes double too.

ABS thresholds versus phase advances are presented in Fig. 14. The asymptotes suggest dependence  $\propto 1/Q_r^2$ . This idea leads to a fitting of Fig. 15, which appears to be rather good. At  $Q_r = 1$  and sufficiently high decrements,  $\alpha\tau_b \gg 3$ , this dependence is of the same scaling as our GP result for the high-intensity threshold, being about half that result. For  $Q_r = 1$ , the same scaling was suggested by B. Zotter [5] and by E. Metral, Ref. [6], with different numerical factors. Zotter's and Metral's thresholds are  $\sim 3 - 4$  times larger than our ABS asymptotic value, correspondingly. This reasonable agreement of the ABS threshold with results of the more realistic GP model without any space charge adds more confidence to the ABS model when it takes the space charge into account, as we do in Ref. [7].

For the accepted SPS impedance model with  $f_r = 1.3$  GHz, the rms bunch length  $\sigma_\tau = 0.77$  ns, and the phase advance  $\nu_r = f_r \sigma_\tau = 1.0$ , the ABS model yields the threshold intensity  $N_p = 4.5 \cdot 10^{11}$ , which amazingly is almost identical to the one obtained by pyHEADTAIL tracking simulations,  $N_p = 4.2 \cdot 10^{11}$  [9, 11]. This number is about 1.5 times below the GP high-intensity threshold, suggesting a rather small Landau damping rate,  $\leq 0.05\omega_s$ , for the tracking conditions. Similarly good agreement is found between the ABS and the HEAD-

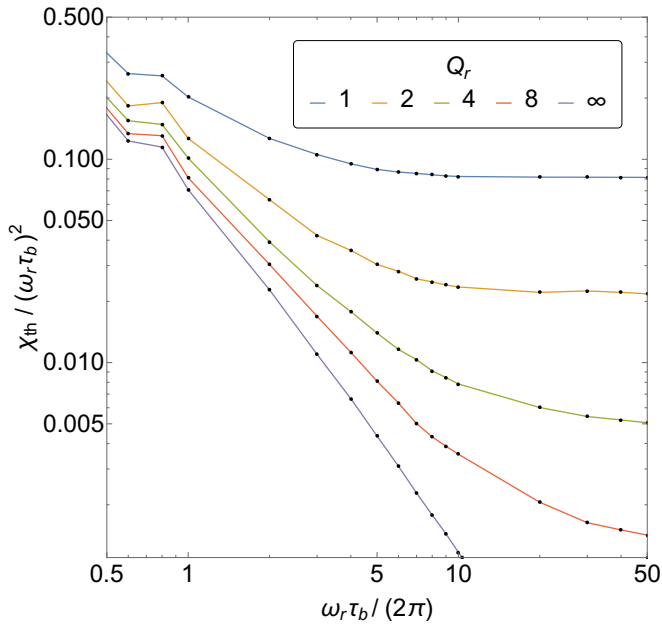


FIG. 14. ABS thresholds versus phase advances for various  $Q$ -factors.

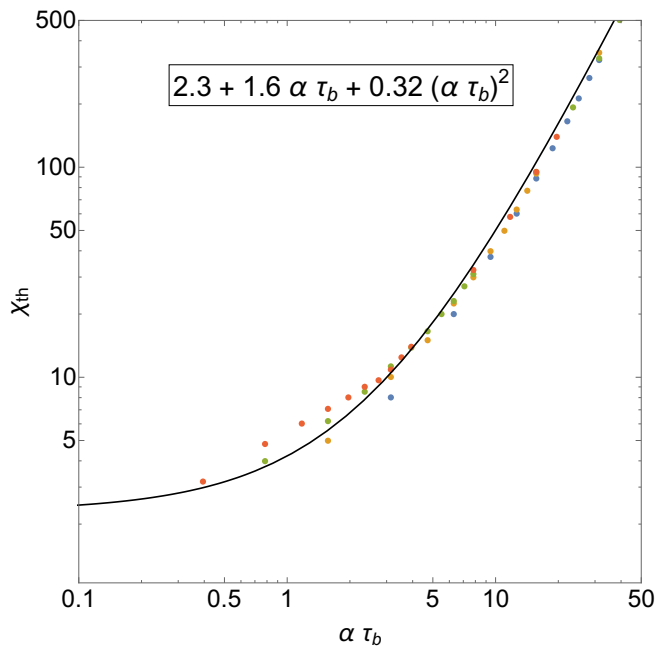


FIG. 15. ABS thresholds can be reasonably fitted by the shown dependence on the wake decrement  $\alpha\tau_b$ . Color convention is the same as in the previous figure.

TAIL tracking simulations for the old Q26 optics [8], giv-

ing the same threshold intensity  $N_p = 1.8 \cdot 10^{11}$ , although the coupling mode numbers are not the same.

#### IV. SUMMARY

Transverse mode coupling instability has been examined by means of the Nested Head-Tail Vlasov solver (NHT) for a Gaussian bunch in a parabolic bucket (GP model) and the ABS model (Air-Bag, Square well) for high-frequency resonator wakes,  $f_r \sigma_\tau \geq 1$ , with various phase advances  $f_r \sigma_\tau$  and decrements  $\alpha_r \sigma_\tau$ . For the GP case, it has been found, in agreement with Ref. [3, 4], that radial modes make the very concept of this threshold rather vague, due to multiple couplings and decouplings of various modes, with a gradually increasing growth rate. Thus, for high-frequency resonator wakes, the instability onset cannot be regularly predicted with good accuracy, unless Landau damping is taken into account. An appreciable agreement was seen between the NHT results and the HEADTAIL and pyHEADTAIL multiparticle simulations for the SPS broadband impedance model, [8, 9, 11]: the same modes -2 and -3 couple at almost the same bunch intensities. It can be said that an amazingly good agreement was found between the ABS threshold and the tracking results: the thresholds do not differ by more than  $\sim 10$ – $15\%$ ; however, the coupling mode numbers are not the same. A fit for the high-intensity threshold of the GP bunch with the broadband impedance,  $Q_r = 1$ , was suggested, being  $\sim 2$  times lower than the analytical predictions of B. Zotter [5] and E. Metral [6]. The same high-frequency scaling law was obtained for the ABS model, with the numerical coefficient about half our high-intensity GP threshold.

#### ACKNOWLEDGMENTS

We are thankful to Adrian Oeftiger for explanations about multiple details of his pyHEADTAIL tracking simulations for the SPS instability. We express our special gratitude to Elias Metral for numerous informative and clarifying discussions.

This manuscript has been authored by Fermi Research Alliance, LLC under Contract No. DE-AC02-07CH11359 with the U.S. Department of Energy, Office of Science, Office of High Energy Physics. The U.S. Government retains and the publisher, by accepting the article for publication, acknowledges that the U.S. Government retains a non-exclusive, paid-up, irrevocable, world-wide license to publish or reproduce the published form of this manuscript, or allow others to do so, for U.S. Government purposes.

- [1] A. Burov, Phys. Rev. ST Accel. Beams **17**, 021007 (2014).
- [2] A. Burov, Phys. Rev. Accel. Beams **19**, 084402 (2016).

- [3] B. Salvant, *Impedance model of the CERN SPS and aspects of LHC single-bunch stability*, Ph.D. thesis, CERN (2010).

- [4] H. Bartosik, *Beam dynamics and optics studies for the LHC injectors upgrade*, Ph.D. thesis, TU Vienna (2013-10-23).
- [5] B. Zotter, *Transverse mode coupling and head-tail turbulence*, Tech. Rep. (1982).
- [6] E. Metral, in *ECLOUD'02: Mini-workshop on electron-cloud simulations for proton and positron beams*, CERN, Geneva, Switzerland, 15-18 Apr 2001: *Proceedings* (2002) pp. 211–218.
- [7] T. Zolkin, A. Burov, and B. Pandey, (2017), arXiv:1711.11110 [physics.acc-ph].
- [8] D. Quatraro and G. Rumolo, *Proceedings, 1st International Particle Accelerator Conference (IPAC'10): Kyoto, Japan, May 23-28, 2010*, Tech. Rep. (2010).
- [9] A. Oeftiger, private communication (2018).
- [10] E. Metral, D. Amorim, S. Antipov, N. Biancacci, X. Bufat, and K. Li, *Proceedings, IPAC'18: Vancouver, Canada, 2018*, Conf. Proc. (2018).
- [11] E. Metral, *Space Charge 2017 Workshop, Darmstadt, Germany*, (2017).
- [12] J.-L. Laclare, *Bunched beam coherent instabilities*, Tech. Rep. (1987).
- [13] M. Blaskiewicz, *Physical Review Special Topics-Accelerators and Beams* **1**, 044201 (1998).